ЖУРНАЛ СТРУКТУРНОЙ ХИМИИ

2016. Том 57, № 1 *Январь – февраль* *С. 80 – 93*

UDC 548.737:543.422

VIBRATIONAL ANALYSIS, CONFORMATIONAL STABILITY, FORCE CONSTANTS, INTERNAL ROTATION BARRIERS, MP2=FULL AND DFT CALCULATIONS OF 1,3-DIMETHYLURACIL TAUTOMERS

U.A. Soliman

Department of Chemistry, Faculty of Science (boys), Al Azhar University, Nasr City, Cairo, Egypt
E-mail: usama_a_soliman@hotmail.com

Received May, 30, 2014 *Revised September, 30, 2014*

The molecular structure of 1,3-dimethyluracil ($C_6H_8N_2O_2$; 1,3-DMU) is studied theoretically and experimentally using Gaussian 98 calculations and different spectroscopic techniques. The vibrational spectrum for 1,3-DMU in the solid phase is recorded in the IR range 4000—400 cm^{-1}. Initially, in order to get the most stable structure, twelve structures were proposed for the titled compound as a result of the internal rotation of CH_3 around C—N bonds and keto-enol tautomerism. The single point energy and frequency calculations are obtained by MP2 (Full) and DFT/B3LYP methods with the 6-31G(*d*) basis set using the Gaussian 98 computation package. After the complete relaxation of twelve isolated isomers, the (*diketo*) tautomer was the only favored structure owing to its low energy relative to the other isomers and the prediction of real frequencies. This interpretation is supported by the recorded infrared spectrum that shows the presence of only the *diketo* tautomer. Aided by the normal coordinate analysis and potential energy distributions, a confident vibrational assignment of the fundamental frequencies is calculated. The results are discussed herein and compared with similar molecules whenever possible.

DOI: 10.15372/JSC20160109

K e y w o r d s: 1,3-dimethyluracil, normal coordinate analysis, vibrational frequencies, *ab initio* calculation, internal rotation barriers.

INTRODUCTION

Uracil is one of the consequential derivatives of pyrimidine, which are known for their biological and pharmaceutical importance [1]. They belong to the family of pyrimidine bases that are of great interest since they control the protein formation and cell functions in living organisms [2, 3] and also due to the important role of N-hetero cyclic molecules (i.e., cytosine, uracil, thymine, etc.) in the structural problems of nucleic acid. The insight into substituted pyrimidines has gained considerable attention [4—6]. Only two purines (adenine, guanine) and three pyrimidines (cytosine, thymine, and uracil) occur widely in nucleic acids [7]. In RNA, uracil base pairs with adenine replace thymine during DNA transcription. In recent times, pyrimidine derivatives have been used in chemotherapy of AIDS and it has also found wide applications as a cancer agent [8]. The number of studies on the vibrational spectroscopy of pyrimidine reported after the publication of the keystone papers by Ito et al. [9] and Lord, Marston, and Miller [10] has considerably increased [11]. Moreover, *keto* pyrimidine derivatives theoretically possessing *keto-enol* tautomerism have been extensively investigated [12, 13].The *keto* form predominates at the equilibrium for most ketones [14], while uracil and its derivatives are found only in the diketo form, as follows from the X-ray crystallographic data [15, 16]. The

experimental data testify that the diketo form of uracils dominates in the gas phase [17—19]. However, the *enol* formation in the solid phase has previously been described only in a single paper [13]. To the best of our knowledge, the vibrational assignments and the structure of 1,3-DMU seems to be not considered yet. Therefore we have initiated the current investigation to check whether the compound has the *keto-enol* or *diketo* structure.

COMPUTATIONAL DETAILS

***Ab initio* and density functional theory calculations.** For 1,3-dimethyluracil, energy minima with respect to nuclear coordinates were obtained by the simultaneous relaxation of all geometric parameters using the Pulay method [20]. The optimized geometry at the level of restricted Hartree—Fock (RHF) calculations with the 6-31G(*d*) basis set was used as a starting point utilizing Møller Plesset many-body perturbation theory (MP2) with full electron correlation [21] up to the 6-31++G(*d*,*p*) computation level for all possible conformations and tautomers. Furthermore, hybrid density functional theory calculations (DFT) [22, 23] at the Becke3LYP theoretical level [24—26] have also been carried out as a compromise between accuracy and feasibility. Some key structural parameters, rotational constants, dipole moments, as obtained from 6-311+G(*d*,*p*) and 6-31++G(*d*,*p*) basis sets of both MP2 and B3LYP methods for the most stable *diketo* form of conformer **3** are presented in Table 1. Total energies and energy differences between conformer **3** and other conformers in cm^{-1} and kcal/mol were given in Fig. 1. All computational calculations were carried out using LCAO-MO SCF GAUSSIAN 98 *ab initio* calculations [27], while the molecular point group symmetry for the titled compound was constrained to the C_s symmetry for both *diketo* and *keto-enol* rotamers.

Conformational isomerism. *Diketo* 1,3-DMU (Fig. 2, *A*) has four conformations according to the positions of hydrogen atoms of two methyl groups with the C=O moiety, but its *keto-enol* tautomer (Fig. 2, *B*) has eight conformations; four of them as the keto form, with the OH moiety eclipsing the C_5=C_6 bond and the OH moiety eclipsing the N_1=C_6 bond for other tautomers. The *keto-enol* tautomeric forms (**5—12**) were found to be transition states due to the prediction of an imaginary wavenumber, except structure **7** that has a positive frequency but is also excluded due to a high energy difference (60.3 kcal/mol) with *diketo* structure **3** (Fig. 1). Using the DFT and MP2 methods with the 6-31G(*d*) basis set, it was found to have the minimum energy of about 0.31—75.6 kcal/mol and 0.49—77.6 kcal/mol in all cases. The computed structures were visualized and verified using the Gauss View program [28]. The optimized SPs of *keto* 1,3-DMU are compared with its X-ray crystallographic data [16] and also some related compounds [29, 30], as shown in Table 1.

Normal coordinate analysis. A normal coordinate analysis was performed for the titled compound with the C_s symmetry where the vibrational modes are spanned into 31A', 17A'' species which are Raman and IR active. Sixty two independent internal coordinates have been used to form forty eight symmetry coordinates (Supplement, Table 1), using the traditional method of Wilson [31]. The description for S_{24}, S_{27}, S_{28}, S_{42}, S_{45}, and S_{46} (Supplement, Table 1) were taken from [32]. The internal coordinate definitions and the numbering of atoms adopted in the current study are shown in Fig. 2. For the normal coordinate analysis, the following procedure has been used to transform the *ab initio* results into the form required for the iterative normal coordinate program. The Cartesian coordinates obtained for the optimized structures were fed into a G-matrix program where the B-matrix was used to convert the *ab initio* force fields in Cartesian coordinates to a force field in the desired internal coordinates. All the diagonal elements of the obtained force field constants have been assigned scaling factors and fed into a force constant program similar to the one written by Schachtschneider [33].

The unscaled B3LYP and MP2=FULL methods with the 6-31G(*d*) basis set and diagonal force constants with internal coordinate definitions are listed in Table 2. The predicted FCs and vibrational frequencies from QM calculations are larger than their experimental counterparts owing to systematic errors such as electron correlation neglect, implemented method(s), and chosen basis sets [34]. Therefore, scaling factors (SFs) (Table 2) were used to obtain scaled frequencies [35, 36] in close agreement with the observed infrared spectra. We also performed frequency calculations for 1,3DMU and 1,3DMU-d_3 (two deuterated methyl groups CD_3) to isolate the CH_3 rocking, twisting, and wagging modes. Similarly, we implemented frequency calculations for 1,3DMU-d_2 (two deuterated CH groups

Table 1

B3LYP *and* MP2 *structural parameters*[a] *for* 1,3-*dimethyluracil* (*conformer* **3**) *utilizing* 6-31G(*d*), 6-311+G(*d*) *and* 6-31++G(*d*,*p*) *basis sets*

Parameters	X-ray			B3LYP for structure **3**		MP2=full for structure **3**	
	Ref. [16]	Ref. [30]	Ref. [29]	6-311+G(*d*)	6-31++G(*d*,*p*)	6-311+G(*d*)	6-31++G(*d*,*p*)
$r(C_2—N_1)$	1.380	1.341	1.353	1.386	1.387	1.383	1.383
$r(C_2—N_3)$	1.375		1.349	1.386	1.387	1.383	1.383
$r(C_4—N_3)$	1.378	1.341	1.336	1.386	1.387	1.383	1.383
$r(C_4=C_5)$	1.331		1.366	1.364	1.351	1.354	1.353
$r(C_5—C_6)$	1.437	1.397	1.400	1.452	1.453	1.451	1.448
$r(C_6—N_1)$	1.399	1.330	1.360	1.417	1.417	1.412	1.411
$r(C_2=O_7)$	1.225			1.220	1.228	1.226	1.236
$r(C_6=O_8)$	1.227			1.220	1.228	1.226	1.236
$r(N_1—C_9)$	1.463			1.463	1.464	1.459	1.459
$r(C_4H_{17})$	1.00			1.084	1.085	1.086	1.081
$r(C_5H_{18})$	0.92		0.949	1.081	1.081	1.082	1.078
$r(C_9H_{11})$	1.09		0.9797	1.085	1.088	1.086	1.083
$r(C_9H_{12})$	0.93		0.9802	1.090	1.092	1.090	1.086
$r(C_9H_{13})$	0.92		0.9801	1.090	1.092	1.090	1.086
$r(O_7…H_{12})$				2.674	2.677	2.653	2.656
$r(O_7…H_{16})$				2.710	2.709	2.700	2.700
$\angle(C_6N_1C_2)$	124.7	122.52	120.5	124.7	124.6	125.3	125.1
$\angle(N_1C_2N_3)$	116.7		122.4	118.6	118.7	118.6	118.6
$\angle(C_2N_3C_4)$	120.8		117.6	118.6	118.7	118.6	118.6
$\angle(N_3C_4C_5)$	122.4	122.52	121.8	123.4	123.3	123.4	123.3
$\angle(C_4C_5C_6)$	120.4	116.09	119.1	121.0	120.8	120.9	120.9
$\angle(C_5C_6N_1)$	114.9	116.06	118.5	113.6	113.8	113.3	113.5
$\angle(N_1C_2O_7)$	121.8			121.4	121.3	121.5	121.4
$\angle(N_3C_2O_7)$	121.5			120.0	119.9	119.9	120.0
$\angle(N_1C_6O_8)$	119.6			121.4	121.3	121.5	121.4
$\angle(C_5C_6O_8)$	125.5			125.0	124.9	125.2	125.1
$\angle(N_3C_4H_{17})$	113.3			114.9	115.0	115.2	115.1
$\angle(C_5C_4H_{17})$	124.3			121.6	121.7	121.4	121.6
$\angle(C_4C_5H_{18})$	123.4		120.44	121.2	121.3	120.9	120.9
$\angle(C_6C_5H_{18})$	116.2		120.51	117.8	117.8	118.2	118.2
$\angle(C_9N_1C_2)$	116.2			116.6	116.7	116.0	116.2
$\angle(C_9N_1C_6)$	119.1			118.7	118.7	118.7	118.7
$\angle(H_{11}C_9N_1)$	104.1			107.4	107.2	107.4	107.0
$\angle(H_{12}C_9N_1)$	112.2			110.1	110.0	109.9	109.6
$\angle(H_{13}C_9N_1)$	112.3			110.1	110.0	109.9	109.6
$\angle(H_{11}C_9H_{12})$	97.0		109.53	110.4	110.7	110.6	110.9
$\angle(H_{11}C_9H_{13})$	103.8		109.53	110.4	110.7	110.6	110.9
$\angle(H_{12}C_9H_{13})$	126.1		109.42	108.4	108.4	108.5	108.8
$\tau\ H_{13}C_9N_1C_2$	–56.9			–59.7	–59.6	–59.6	–59.7
$\tau\ H_{15}C_{10}N_3C_2$	59.5			59.9	59.8	59.8	59.9
A, MHz				2239	2232	2247	2244
B, MHz				1310	1306	1311	1308
C, MHz				835	832	836	835
μ_{tot}, Debye				4.415	4.479	4.949	5.057

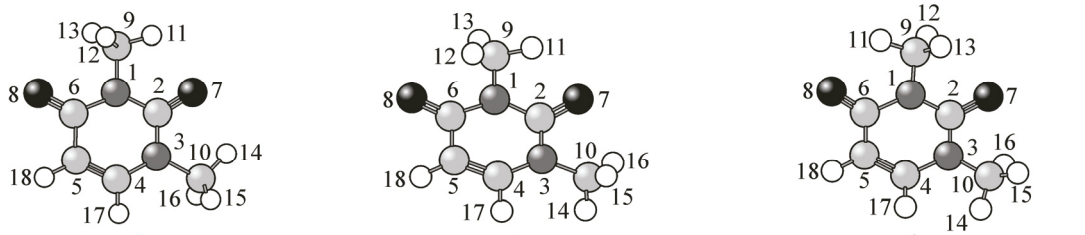

1
ΔE = 388 cm^{-1}(0.97 kcal mol^{-1})
417 **cm^{-1}(*1.2* kcal mol^{-1})**

2
ΔE = 145 cm^{-1}(0.41 kcal mol^{-1})
144 **cm^{-1}(*0.41* kcal mol^{-1})**

3
Minimum

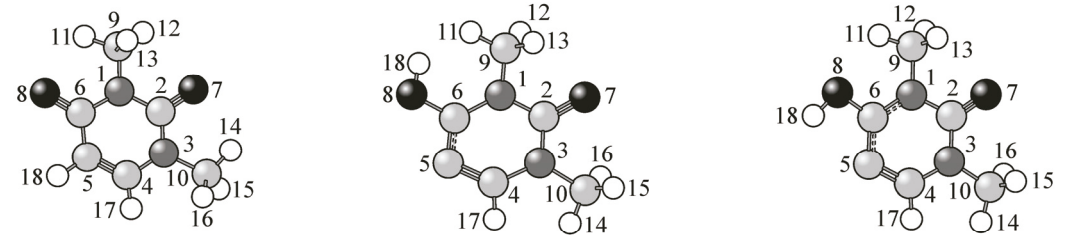

4
ΔE = 108 cm^{-1}(0.31 kcal mol^{-1})
172 **cm^{-1}(*0.49* kcal mol^{-1})**

5
ΔE = 21233 cm^{-1}(60.7 kcal mol^{-1})
21358 **cm^{-1}(*61.1* kcal mol^{-1})**

6
ΔE = 26490 cm^{-1}(75.7 kcal mol^{-1})
27179 **cm^{-1}(*77.7* kcal mol^{-1})**

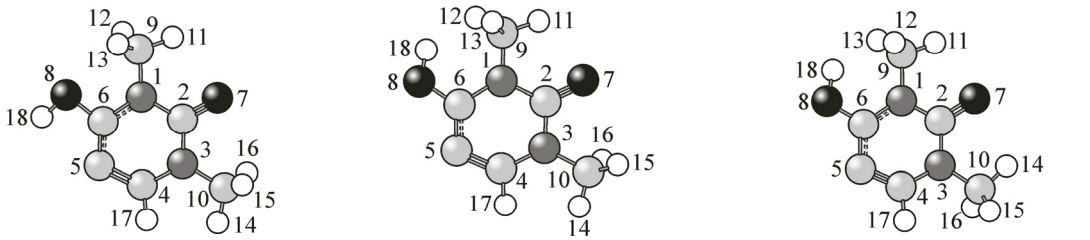

7
ΔE = 20790 cm^{-1}(59.4 kcal mol^{-1})
21092 **cm^{-1}(*60.0* kcal mol^{-1})**

8
ΔE = 25316 cm^{-1}(72.7 kcal mol^{-1})
26025 **cm^{-1}(*74.3* kcal mol^{-1})**

9
ΔE = 25434 cm^{-1}(72.7 kcal mol^{-1})
26035 **cm^{-1}(*74.3* kcal mol^{-1})**

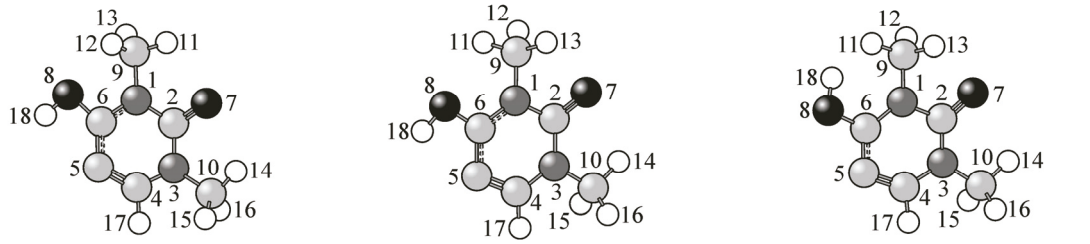

10
ΔE = 20922 cm^{-1}(59.8 kcal mol^{-1})
21279 **cm^{-1}(*60.8* kcal mol^{-1})**

11
ΔE = 21035 cm^{-1}(60.1 kcal mol^{-1})
21418 **cm^{-1}(*61.2* kcal mol^{-1})**

12
ΔE = 26450 cm^{-1}(75.6 kcal mol^{-1})
27149 **cm^{-1}(*77.6* kcal mol^{-1})**

Fig. 1. Total energies and energy differences between conformer **3** and other conformers

CD_2). The predicted harmonic vibrational frequencies, infrared intensities, Raman activities, and PEDs for each fundamental giving the description of each normal mode are presented in Table 3.

Calculated IR and Raman spectra. It has already been accepted that a clear prediction of Raman (R) and infrared (IR) spectra is essential in the vibrational analysis of organic molecules, which makes vibrational spectroscopy a more practical tool [37—41]. The simulated vibrational spectra can be obtained using either IR intensities or Raman activities along with their dipole moments or polarizability derivatives respectively. The frequencies of the *diketo* tautomer were obtained from the calculation by B3LYP and MP2=Full methods with the 6-31G(*d*) basis set. In the calculation of the Raman spectrum, the Raman scattering cross-section is derived from the scattering activities and the predicted frequencies proportional to the Raman intensity for each normal mode [42—44, 36]. To

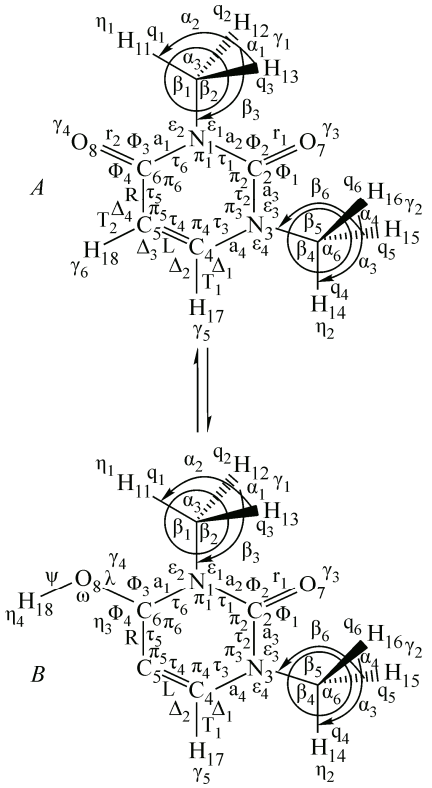

Fig. 2. Internal coordinate definitions and the numbering of atoms

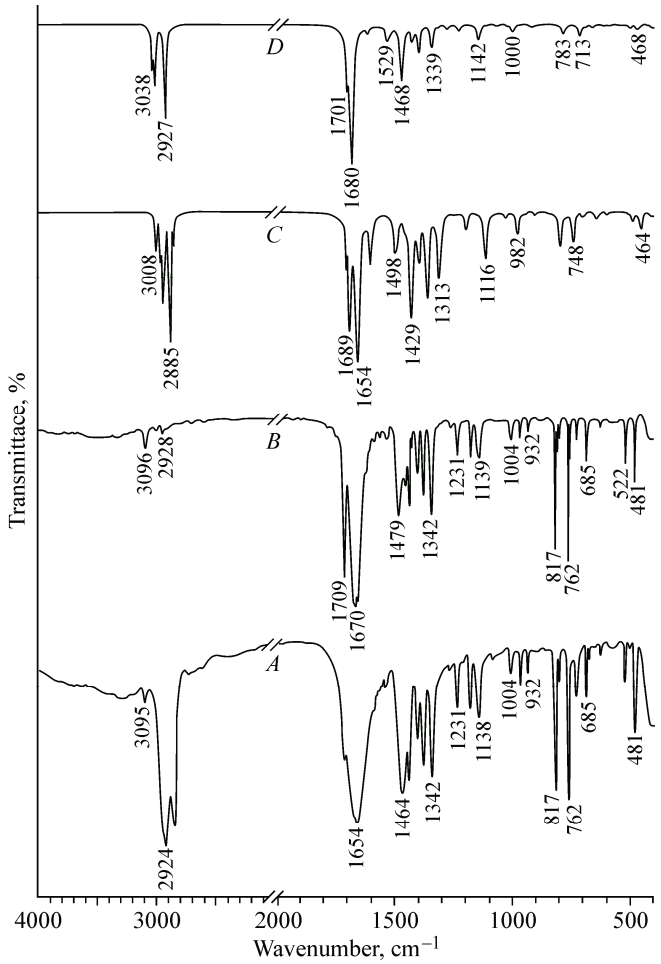

Fig. 3. IR spectrum of 1,3-Dimemyluracil; experimental from 400 to 4000 cm^{-1} in Nujol (*A*); experimental from 400 to 4000 cm^{-1} in KBr (*B*), scaled B3LYP/6-31G(*d*) (*C*); scaled MP2(full)6-31G(*d*) (*D*)

calculate the IR spectrum, derivatives of the dipole moment were taken from the DFT calculation data and transformed to the normal coordinates. To aid in vibrational assignments, we calculated IR spectra (Fig. 3, 4000—400 cm^{-1}) of *diketo* (1,3-DMU) using the fundamental frequencies from B3LYP and MP2=Full calculations with the 6-31G(*d*) basis set. These calculated IR spectra were compared with the experimental IR spectra in KBr disks and in Nujol (Fig. 3, *A*, 3, *B*) taken from [45].

RESULTS AND DISCUSSION

Structural parameters and force constants. It is estimated that the heavy atom and carbon-hydrogen distances should be accurate within ±0.023—0.001 Å and ±0.182—0.002 Å respectively. The angles are expected to be accurate within ±0.5—2.6°, for all angles except methyl group angles found to be has less accurate with calculate values within ±0.5—7.3°. Moreover, the dihedral angles were in excellent agreement within ±0.3—0.4°, as compared to the X-ray crystallographic data for 1,3-DMU [16]. The calculated SPs (Table 1) for 1,3DMU reveal that six C—N distances present in the investigated compound are in good agreement with X-ray values for 1,3-DMU, pyrimidine, and 2-amino-4,6-dimethylpyrimidinium 3,5-dinitrobenzoate dihydrate [16, 29, 30]. Also, the C_4=C_5 and C_5—C_6 distances match with those of the X-ray crystallographic data for 1,3-DMU, pyrimidine, and 2-amino-4,6-dimethylpyrimidinium 3,5-dinitrobenzoate dihydrate [16, 29, 30] within 0.035—0.019 Å and 0.057—0.011 Å respectively. It should be mentioned that the predicted values for C_2=O_7 and C_6=O_8

Table 2

B3LYP/6-31G(*d*) *and* MP2=full/6-31G(*d*) *unscaled force constants* (mdyne/Å) *for* 1,3-*dimethyluracil* (*conformer* **3**) *molecule*

Atom #	Vib. modes	Symbol[a]	Scaling factor[b]	Diagonal force constant[c]	Diagonal force constant[d]
1	2	3	4	5	6
N_1—C_6	Stretch	a_1	0.874	4.110	4.436
N_1—C_2	Stretch	a_2	0.874	4.794	5.087
C_2—N_3	Stretch	a_3	0.874	4.711	5.008
N_3—C_4	Stretch	a_4	0.874	4.793	5.138
N_1—C_9	Stretch	a_5	0.874	5.200	5.534
N_3—C_{10}	Stretch	a_6	0.874	5.230	5.552
C_4=C_5	Stretch	L	0.874	6.697	6.861
C_5—C_6	Stretch	R	0.874	4.104	4.385
C_2=O_7	Stretch	r_1	0.874	12.476	12.423
C_6=O_8	Stretch	r_2	0.874	12.392	12.298
C_4H_{17}	Stretch	T_1	0.874	5.680	5.786
C_5H_{18}	Stretch	T_2	0.874	5.826	5.950
C_9H_{11}	Stretch	q_1	0.874	5.622	5.814
C_9H_{12}	Stretch	q_2	0.874	5.390	5.626
C_9H_{13}	Stretch	q_3	0.874	5.390	5.626
$C_{10}H_{14}$	Stretch	q_4	0.874	5.469	5.682
$C_{10}H_{15}$	Stretch	q_5	0.874	5.394	5.621
$C_{10}H_{16}$	Stretch	q_6	0.874	5.394	5.621
$C_6N_1C_2$	Bending	π_1	0.945	0.777	0.793
$N_1C_2N_3$	Bending	π_2	0.945	0.781	0.796
$C_2N_3C_4$	Bending	π_3	0.945	0.696	0.712
$N_3C_4C_5$	Bending	π_4	0.945	0.694	0.711
$C_4C_5C_6$	Bending	π_5	0.945	0.689	0.706
$C_5C_6N_1$	Bending	π_6	0.945	0.702	0.722
$H_{11}C_9N_1$	Bending	β_1	0.945	0.689	0.714
$H_{13}C_9N_1$	Bending	β_2	0.945	0.684	0.705
$H_{12}C_9N_1$	Bending	β_3	0.945	0.684	0.705
$H_{12}C_9H_{13}$	Bending	α_1	0.945	0.503	0.522
$H_{13}C_9H_{11}$	Bending	α_2	0.945	0.499	0.518
$H_{11}C_9H_{12}$	Bending	α_3	0.945	0.499	0.518
$H_{14}C_{10}N_3$	Bending	β_4	0.945	0.694	0.716
$H_{16}C_{10}N_3$	Bending	β_5	0.945	0.685	0.705
$H_{15}C_{10}N_3$	Bending	β_6	0.945	0.685	0.705
$H_{15}C_{10}H_{16}$	Bending	α_4	0.945	0.515	0.534
$H_{16}C_{10}H_{14}$	Bending	α_5	0.945	0.497	0.517
$H_{14}C_{10}H_{15}$	Bending	α_6	0.945	0.497	0.517
$C_9N_1C_2$	Bending	ε_1	0.945	0.760	0.792
$C_9N_1C_6$	Bending	ε_2	0.945	0.805	0.839
$C_{10}N_3C_2$	Bending	ε_3	0.945	0.668	0.684
$C_{10}N_3C_4$	Bending	ε_4	0.945	0.663	0.671
$O_7C_2N_1$	Bending	Φ_1	0.945	0.869	0.865

Continued Table 2

1	2	3	4	5	6
$O_7C_2N_3$	Bending	Φ_2	0.945	0.887	0.885
$O_8C_6N_1$	Bending	Φ_3	0.945	0.882	0.890
$O_8C_6C_5$	Bending	Φ_4	0.945	0.725	0.730
$H_{17}C_4N_3$	Bending	Δ_1	0.945	0.497	0.512
$H_{17}C_4C_5$	Bending	Δ_2	0.945	0.443	0.456
$H_{18}C_5C_4$	Bending	Δ_3	0.945	0.420	0.431
$H_{18}C_5C_6$	Bending	Δ_4	0.945	0.417	0.427
$H_{12}C_9N_1H_{13}$	Wag	γ_1	0.978	0.337	0.341
$H_{15}C_{10}N_3H_{16}$	Wag	γ_2	0.978	0.280	0.272
$N_1C_2O_7N_3$	Wag	γ_3	0.978	0.850	0.849
$N_1C_6O_8C_5$	Wag	γ_4	0.978	0.641	0.624
$N_3C_4H_{17}C_5$	Wag	γ_5	0.978	0.480	0.458
$C_4C_5H_{18}C_6$	Wag	γ_6	0.978	0.429	0.414
$H_{11}C_9N_1C_2$	Torsion	η_1	0.978	0.003	0.003
$H_{14}C_{10}N_3C_2$	Torsion	η_2	0.978	0.001	0.001
$C_6N_1C_2N_3$	Puckering	τ_1	0.978	0.097	0.101
$N_1C_2N_3C_4$	Puckering	τ_2	0.978	0.089	0.092
$C_2N_3C_4C_5$	Puckering	τ_3	0.978	0.142	0.144
$N_3C_4C_5C_6$	Puckering	τ_4	0.978	0.171	0.172
$C_4C_5C_6N_1$	Puckering	τ_5	0.978	0.110	0.106
$C_5C_6N_1C_2$	Puckering	τ_6	0.978	0.092	0.090

[a] See Fig. 2 for atom numbering and internal coordinates definitions.
[b] Implemented scaling factors to reproduce scaled frequencies in Table 3.
[c] Diagonal force constant at B3LYP/6-31G(*d*) level.
[d] Diagonal force constant at MP2=full/6-31G(*d*) level.

distances are in close proximity to those provided by the X-ray crystallographic data (Table 1) within 0.005—0.007 Å [16, 29, 30]. This refers to the absence of the *keto-enol* form as reported previously [12, 13, 15, 17—19]. Moreover, the calculated O---H bond lengths range from 2.236 Å to 2.710 Å, which is smaller than the sum of Van der Waal radii of oxygen and hydrogen atoms (2.72 Å) by 0.464—0.01 Å [46, 47]. Therefore, moderate intramolecular hydrogen bonding interactions are predicted between O_8---H_{11}, O_8---H_{18}, O_7---H_{12}, and O_7---H_{16} in addition to the expected intermolecular hydrogen interactions in 1,3-DMU (Table 1).

Internal rotation barriers. A potential surface scan (PSS) for the internal rotation of methyl in the most stable conformers of 1,3-DMU (structure **3**) has been predicted from *ab initio* MP2=full calculations utilizing the standard 6-311++G(*d*,*p*) basis set. For this purpose, the dihedral angle of the —CH_3 group (τ $H_{11}C_9N_1C_6$) was allowed to vary from 0° to 180° by 10° increments while the structural parameters were held fixed to the MP2(full)/6-311++G(*d*,*p*) optimized values for structure **3**. As can be concluded from the produced PSS curve (Fig. 4), the calculated energy of structure **3** (E = = –492.09894 Hartree) is found to increase as the dihedral angle (τ $H_{11}C_9N_1C_6$) is rotated by 10° increments until a maximum (E = –492.09737 Hartree) is reached at 60° with an energy barrier of 345 cm^{-1} (0.98 kcal/mol). After that, the energy decreases, reaching a local minimum at 140° with an energy barrier of 101 cm^{-1} (0.29 kcal/mol) relative to most stable structure **3**. The continued rotation of the dihedral angle results in a decrease in the energy until reaching a local maximum at 180° (structure **2**). The estimated barriers for 1,3-DMU methyl seem to be consistent with the calculated values of

Table 3

Observed and calculated frequencies (cm^{-1}) *for* 1,3-*dimethyl uracil* (1,3DMU) *structure* **3** *diketo form*

Species	ν_i*	Assignment[a]	B3LYP/6-31G(*d*)					Obs. (this study)[g]	
			Fixed[b] scaled	(X—D)[c]	IR Int[d].	Raman Act[e].	PED[f]	IR solid (KBr)	IR solid (Nujol)
1	2	3	4	5	6	7	8	9	10
A′	ν_1	υ_s CH/CD	3051	2419	0.54	114.8	$67S_1 33S_2$	3096w	3095w
	ν_2	υ_s CH/CD	3008	2378	7.4	83.7	$67S_2 32S_1$	(3004w)	(2955vs)
	ν_3	υ_{as} CH_3/CD_3	3000	2381	0.61	31.0	$48S_3 48S_4$	(3004w)	(2955vs)
	ν_4	υ_{as} CH_3/CD_3	2966	2356	8.5	50.7	$50S_4 49S_3$	2961w	(2955vs)
	ν_5	υ_s CH_3/CD_3	2885	2214	22.3	122.5	$51S_5 44S_6$		(2854s)
	ν_6	υ_s CH_3/CD_3	2880	2209	32.6	135.1	$53S_6 46S_5$		(2854s)
	ν_7	υ_s C=O	1689		170.4	37.4	$79S_7$	1709vs	1708vs
	ν_8	υ_s C=O	1654		780.1	13.6	$73S_8$	1670vs	1670vs
	ν_9	υ_s C=C Ring	1600		53.1	13.0	$56S_9 12S_{14} 10S_8$	1616s	
	ν_{10}	δ_{ip} CH_3/CD_3	1498	1141	32.6	22.6	$51S_{10} 24S_{11} 10S_{20}$	(1479s)	(1464s)
	ν_{11}	δ_{ip} CH_3/CD_3	1488	1129	12.1	14.0	$57S_{11} 20S_{12}$	(1479s)	(1464s)
	ν_{12}	$\delta_{Umbrella}$ CH_3/CD_3	1444	1101	6.8	2.6	$51S_{12} 26S_{13}$	1448w	
	ν_{13}	$\delta_{Umbrella}$ CH_3/CD_3	1429	1086	145.8	0.77	$16S_{13} 15S_{12} 12S_{10} 10S_{14} 10S_{17} 10S_{22} 10S_{27}$	1434s	1436s
	ν_{14}	δ_{ip} CH/CD	1397	925	44.8	11.4	$11S_{14} 48S_{13} 10S_{16} 10S_{19}$	1399m	1398m
	ν_{15}	υ_s C—N ring	1361		104.6	16.0	$19S_{15} 26S_{12} 10S_{14} 10S_{19} 10S_{23}$	1376s	1376s
	ν_{16}	υ_s C—N ring	1313		75.9	0.36	$20S_{16} 28S_{14} 10S_{10} 10S_{15} 10S_{20}$	1342s	1342s
	ν_{17}	υ_s C—N ring	1244		1.4	21.3	$35S_{17} 25S_{21} 10S_{20} 10S_{31}$	1231m	1231m
	ν_{18}	υ_s C—N	1198		17.7	3.2	$49S_{18} 19S_{24} 13S_{25}$	1174m	1174m
	ν_{19}	δ_{ip} CH/CD	1157	842	1.3	10.8	$50S_{19} 10S_9 10S_{21} 10S_{22} 10S_{23}$	1145w	1146w
	ν_{20}	ρ CH_3/CD_3	1116	870	50.4	3.3	$27S_{20} 19S_{22} 17S_{14} 10S_{29}$	(1139m)	(1138m)
	ν_{21}	ρ CH_3/CD_3	1032	834	4.5	2.8	$30S_{21} 33S_{17} 28S_{23}$	1004w	1004w
	ν_{22}	υ_s C—C ring	982		21.7	1.6	$13S_{22} 35S_{20} 23S_{16} 10S_{23}$	955w	955w
	ν_{23}	υ_s C—N	907		2.0	3.0	$26S_{23} 14S_{15} 11S_{21} 10S_{17} 10S_{24} 10S_{26}$	(932w)	(932w)
	ν_{24}	Ring bending	780		1.8	6.2	$50S_{24} 10S_7 10S_{18} 10S_{22}$	799w	798w
	ν_{25}	υ_s C—N ring	649		6.0	17.6	$46S_{25} 20S_{18} 10S_{22} 10S_{28}$	685w	686m
	ν_{26}	δ_{ip} C=O	608		1.1	0.49	$20S_{26} 32S_{29} 13S_{22} 11S_{31} 10S_{15}$	602w	605w
	ν_{27}	Ring bending	496		8.8	5.0	$51S_{27} 11S_{15} 10S_{24} 10S_{26}$	522m	523m
	ν_{28}	Ring bending	464		14.8	8.0	$56S_{28} 10S_{15} 10S_{18} 10S_{25}$	481s	481s
	ν_{29}	δ_{ip} C=O	396		25.2	0.49	$39S_{29} 12S_{26} 11S_{15} 11S_{28} 10S_{27}$		
	ν_{30}	N_1—C_9 bending	353		12.2	0.12	$47S_{30} 20S_{26} 18S_{21} 10S_{28}$		
	ν_{31}	N_3—C_{10} bending	299		1.7	0.29	$55S_{31} 23S_{30}$		
A″	ν_{32}	υ_{as} CH_3/CD_3	2945	2338	11.3	78.7	$52S_{32} 48S_{33}$	(2928w)	(2924vs)
	ν_{33}	υ_{as} CH_3/CD_3	2943	2336	13.2	58.8	$52S_{33} 48S_{32}$	(2928w)	(2924vs)
	ν_{34}	δ_{as} CH_3/CD_3	1481	1100	8.6	16.2	$47S_{34} 46S_{35}$	(1464w)	
	ν_{35}	δ_{as} CH_3/CD_3	1457	1081	7.2	19.9	$46S_{35} 45S_{34}$	(1464w)	
	ν_{36}	ρ CH_3/CD_3	1137	913	0.32	3.0	$60S_{36} 31S_{37}$	(1139m)	(1138m)
	ν_{37}	ρ CH_3/CD_3	1128	904	0.19	2.3	$60S_{37} 31S_{36}$	(1139m)	(1138m)
	ν_{38}	γ_{wag} CH/CD	954	777	0.86	1.0	$89S_{38} 10S_{39}$	(932w)	(932w)
	ν_{39}	γ_{wag} CH/CD	802	582	34.7	1.9	$57S_{39} 37S_{41}$	817vs	817

Continued Table 3

1	2	3	4	5	6	7	8	9	10
	ν_{40}	γ_{wag} C=O	748		29.4	0.23	$83S_{40}14S_{41}$	762s	762vs
	ν_{41}	γ_{wag} C=O	707		3.1	4.0	$36S_{41}18S_{40}16S_{39}16S_{42}$	728w	722w
	ν_{42}	δ Ring puckering	428		0.65	1.7	$35S_{42}42S_{45}11S_{41}10S_{44}$		474m
	ν_{43}	δ_{OOP} N_1—C_9	252		0.49	0.74	$39S_{43}40S_{44}10S_{42}$		
	ν_{44}	δ_{OOP} N_3—C_{10}	198		3.0	0.82	$54S_{44}45S_{43}$		
	ν_{45}	τ CH_3/CD_3	125	76	8.0	0.02	$41S_{45}41S_{47}15S_{42}$		
	ν_{46}	τ CH_3/CD_3	114	52	0.16	0.23	$81S_{46}10S_{47}$		
	ν_{47}	δ Ring puckering	98		3.7	0.89	$34S_{47}44S_{45}25S_{42}$		
	ν_{48}	δ Ring puckering	66		0.64	0.12	$96S_{48}$		

Species	ν_i^*	Assignment[a]	MP2(full)/6-31G(*d*)				
			Fixed scaled	(X—D)[c]	IR Int[d].	Raman Act[e].	PED[f]
1	2	3	4	5	6	7	8
A′	ν_1	υ_s CH/CD	3084	2447	0.97	103.0	$65S_134S_2$
	ν_2	υ_s CH/CD	3038	2402	8.8	99.2	$56S_229S_110S_4$
	ν_3	υ_{as} CH_3/CD_3	3058	2428	0.36	27.0	$49S_349S_4$
	ν_4	υ_{as} CH_3/CD_3	3031	2408	1.7	22.8	$43S_442S_310S_2$
	ν_5	υ_s CH_3/CD_3	2934	2251	16.7	94.4	$49S_548S_6$
	ν_6	υ_s CH_3/CD_3	2927	2245	25.8	116.2	$50S_650S_5$
	ν_7	υ_s C=O	1701		167.6	73.6	$73S_7$
	ν_8	υ_s C=O	1680		726.6	23.5	$61S_810S_910S_{16}$
	ν_9	υ_s C=C Ring	1614		19.2	9.2	$48S_919S_811S_{14}10S_{15}$
	ν_{10}	δ_{ip} CH_3/CD_3	1529	1163	41.6	21.5	$50S_{10}25S_{11}10S_{20}$
	ν_{11}	δ_{ip} CH_3/CD_3	1519	1148	14.1	11.2	$58S_{11}21S_{10}10S_{21}$
	ν_{12}	$\delta_{Umbrella}$ CH_3/CD_3	1458	1125	7.1	3.2	$48S_{12}28S_{13}$
	ν_{13}	$\delta_{Umbrella}$ CH_3/CD_3	1423	1109	44.1	6.0	$58S_{13}10S_{12}10S_{14}10S_{16}$
	ν_{14}	δ_{ip} CH/CD	1339	938	70.6	2.2	$35S_{14}18S_{16}10S_{10}10S_{15}10S_{20}$
	ν_{15}	υ_s C—N ring	1396		86.7	26.8	$20S_{15}26S_{12}11S_{14}11S_{19}10S_910S_{23}$
	ν_{16}	υ_s C—N ring	1468		195.4	2.8	$10S_{16}14S_{12}13S_{10}10S_{15}10S_{17}10S_{22}10S_{25}10S_{27}$
	ν_{17}	υ_s C—N ring	1276		10.2	38.9	$41S_{17}20S_{21}10S_{11}10S_{16}$
	ν_{18}	υ_s C—N	1224		19.3	1.3	$50S_{18}17S_{24}12S_{25}$
	ν_{19}	δ_{ip} CH/CD	1177	855	0.07	13.9	$50S_{19}10S_{21}10S_{22}10S_{23}$
	ν_{20}	ρ CH_3/CD_3	1142	883	46.8	3.3	$30S_{20}19S_{14}16S_{22}10S_{23}$
	ν_{21}	ρ CH_3/CD_3	1065	847	3.2	4.7	$37S_{21}27S_{17}27S_{23}$
	ν_{22}	υ_s C—C ring	1000		24.1	1.4	$13S_{22}34S_{20}22S_{16}10S_{23}$
	ν_{23}	υ_s C—N	924		2.4	2.8	$26S_{23}15S_{15}11S_{21}10S_{17}10S_{24}10S_{26}$
	ν_{24}	Ring bending	786		2.1	6.4	$52S_{24}10S_710S_{18}10S_{22}$
	ν_{25}	υ_s C—N ring	660		5.6	18.1	$50S_{25}20S_{18}10S_{22}$
	ν_{26}	δ_{ip} C=O	611		1.6	1.5	$21S_{26}32S_{29}12S_{22}12S_{31}10S_{15}$
	ν_{27}	Ring bending	500		7.9	5.3	$53S_{27}11S_{15}10S_{16}10S_{26}$
	ν_{28}	Ring bending	468		12.2	8.5	$57S_{28}10S_{15}10S_{18}10S_{25}$
	ν_{29}	δ_{ip} C=O	398		22.7	0.69	$42S_{29}10S_{15}10S_{26}10S_{27}10S_{28}10S_{30}$
	ν_{30}	N_1—C_9 bending	358		14.8	0.11	$46S_{30}24S_{26}14S_{31}12S_{28}$
	ν_{31}	N_3—C_{10} bending	304		1.6	0.21	$58S_{31}20S_{30}10S_{16}$

Continued Table 3

1	2	3	4	5	6	7	8
A″	ν_{32}	υ_{as} CH_3/CD_3	3015	2394	9.9	56.4	$49S_{32}51S_{33}$
	ν_{33}	υ_{as} CH_3/CD_3	3014	2394	5.4	59.9	$49S_{33}51S_{32}$
	ν_{34}	δ_{as} CH_3/CD_3	1512	1124	9.2	14.5	$48S_{34}46S_{35}$
	ν_{35}	δ_{as} CH_3/CD_3	1488	1105	7.5	18.9	$47S_{35}46S_{34}$
	ν_{36}	ρ CH_3/CD_3	1156	927	0.32	3.6	$62S_{36}31S_{37}$
	ν_{37}	ρ CH_3/CD_3	1147	914	0.33	2.6	$62S_{37}31S_{36}$
	ν_{38}	γ_{wag} CH/CD	912	734	4.1	1.0	$89S_{38}$
	ν_{39}	γ_{wag} CH/CD	783	580	30.2	1.7	$67S_{39}25S_{41}$
	ν_{40}	γ_{wag} C=O	713		33.2	2.0	$99S_{40}$
	ν_{41}	γ_{wag} C=O	690		5.1	2.1	$68S_{4}20S_{42}$
	ν_{42}	δ Ring puckering	410		1.2	1.3	$41S_{42}42S_{45}$
	ν_{43}	δ_{OOP} N_1—C_9	244		0.11	0.82	$37S_{43}47S_{44}16S_{42}$
	ν_{44}	δ_{OOP} N_3—C_{10}	189		5.0	0.85	$53S_{44}50S_{43}$
	ν_{45}	τ CH_3/CD_3	128	68	6.5	0.04	$35S_{45}30S_{48}24S_{42}$
	ν_{46}	τ CH_3/CD_3	114	59	0.28	0.19	$97S_{46}$
	ν_{47}	δ Ring puckering	92		1.4	0.88	$42S_{47}45S_{45}$
	ν_{48}	δ Ring puckering	66		1.8	0.06	$20S_{48}24S_{42}22S_{46}15S_{47}$

[a] Notations for fundamentals: m, stretch; d, bending; c, wagging; R, ring and s, torsion. These fundamentals could be pure in minor cases; however they are coupled with other normal modes as given in PEDs.

[b] Scaling factors 0.874 for all stretches and 0.945 for bends and 0.978 for wags and torsions.

[c] The calculated unscaled frequencies for d_1-1,3DMU (X—D=C—D) and d_3-1,3DMU (X—D=C—D_3) isotopmers.

[d] Calculated infrared intensities in km/mol (IUPAC, Glossary of terms used in Photochemistry, 3rd Edition, July 2004).

[e] Calculated Raman activities in $Å^4$/amu.

[f] Contributions less than 10 % are omitted.

[g] Bands between brackets are used for two or three normal modes of vibration.

395 cm^{-1} for 4-bromo-*o*-xylene [48] and 392 cm^{-1} for 1,1,1-trifluoroacetone [49]. Furthermore, three-dimensional PSS for 1,3-DMU was predicted by the simultaneous rotation of both methyl groups ($\tau_1 = \tau H_{11}C_9N_1C_6$ and $\tau_2 = \tau H_{14}C_{10}N_3C_2$). On the potential surface shown in (Fig. 5), the global minimum with $\tau_1 = 0.0$ and $\tau_2 = 180°$ corresponds to the most stable conformer (structure **3**).

Vibrational assignments. The frequencies calculated by the DFT methods are in better agreement with the experimental frequencies than the MP2(full) ones (Table 3). This suggests that the DFT methods incorporate some anharmonic contributions, which improve the correlation with the experiment. So the proposed vibrational assignment presented herein is based on the B3LYP/6-31G(*d*) frequencies compared to the observed IR wavenumbers.

C—H vibrations. The hetero aromatic structure showing the presence of C—H asymmetric stretching vibrations in the range 3100—2950 cm^{-1} is suggested for symmetric stretching modes of vibrations [50—53]. In this range, the bands are not appreciably affected by the nature of the substituents. Hence, in the present investigation, the obs/calc IR bands at 3096/3051 cm^{-1} and 3004/3008 cm^{-1} have been assigned to C—H stretching vibrations. In general, in-plane and out-of-plane heteroaromatic C—H bending vibrations occur in the ranges 1300—1000 cm^{-1} and 600—1000 cm^{-1} respectively [12, 54]. Hence in the present investigation, the C—H in-plane bending vibrations (ν_{14} and ν_{19}) computed at 1397 cm^{-1} and 1157 cm^{-1} by the B3LYP/6-31G***** method show good agreement with IR observed bands at 1399 cm^{-1} and 1145 cm^{-1} respectively. While the observed bands

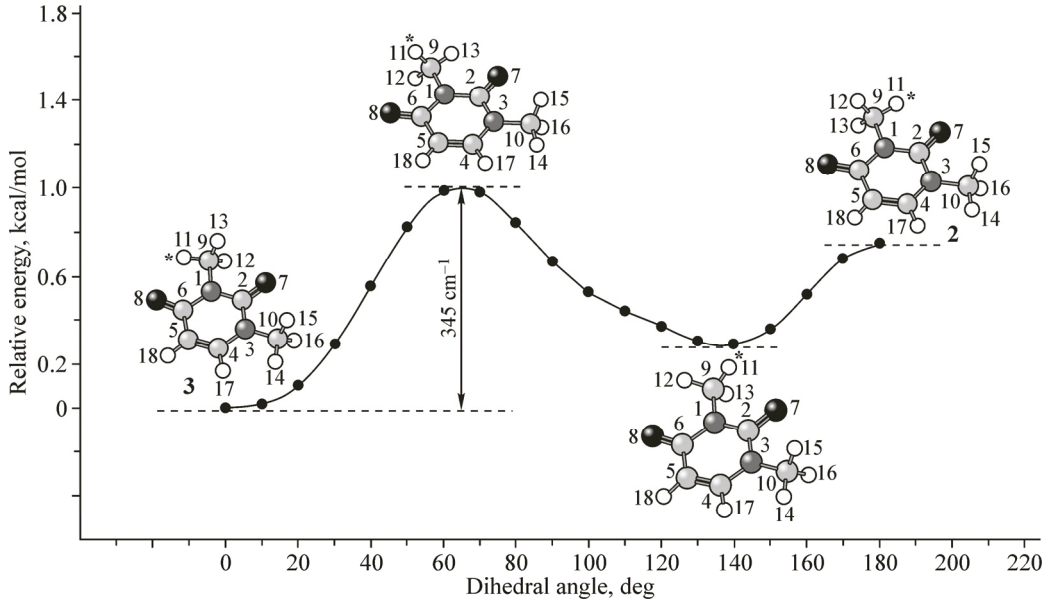

Fig. 4. Methyl barriers to internal rotation of 1,3-Dimethyluracil as obtained from MP2(full)/6-31++G(*d*,*p*) potential surface scan. The rotation started from the hydrogen atom marked with asterisk; H_{11}

in the IR spectrum at 932 cm^{-1} and 817 cm^{-1} match those calculated at 954 cm^{-1} (ν_{38}) and 802(ν_{39}) cm^{-1} by the B3LYP/6-31G* method. These bands are assigned to the C—H out-of-plane bending vibration. These observations were in good agreement with the experimental as well as literature data [55].

CH_3 fundamental vibrations. The CH_3 anti-symmetric stretching is expected around 2980 cm^{-1} and the symmetric stretching is expected at 2870 cm^{-1} [56]. The predicted band at 3000 cm^{-1} (ν_3) was matched with the observed weak IR band at 3004 cm^{-1}. In line with this, the peaks observed in the IR spectrum at 2961 cm^{-1} and 2928 cm^{-1} were assigned to CH_3 asymmetric stretching vibrations whereas symmetric stretching modes were not observed (Fig. 3, *B*), but appear at 2854 cm^{-1} in the Nujol IR

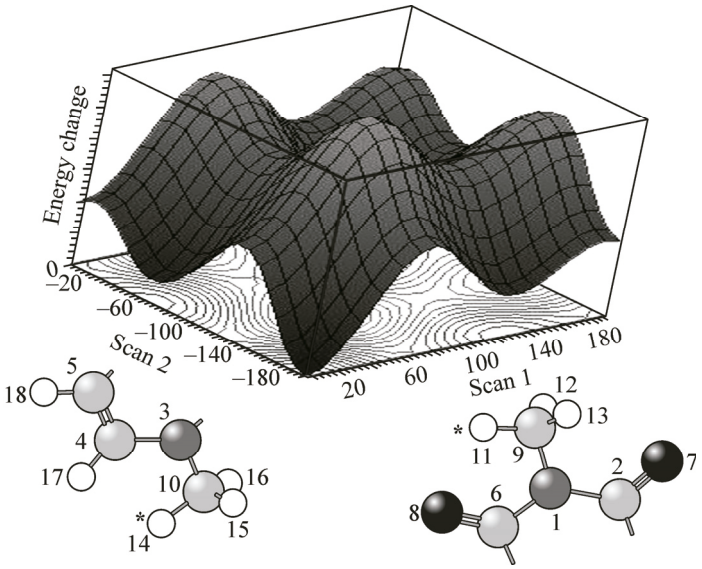

Fig. 5. Three dimention methyl barrier to internet rotation of 1,3-Dimethyl-uracil as obtained from MP2(full)/6-31++G(*d*,*p*) potential surface scan. The rotation started from the hydrogen atom marked with asterisk

spectrum (Fig. 3, *A*, Table 3). These assignments correlate with the calculated bands at 3000 cm^{-1}, 2966 cm^{-1} and 2945 cm^{-1}, 2943 cm^{-1} for the asymmetric stretch and 2885 cm^{-1}, 2880 cm^{-1} for the symmetric stretch obtained by the B3LYP/6-31G* method, respectively. These assignments agree well with the literature values [57—59]. From the other point of view the CH_3 symmetric and asymmetric in-plane bending modes appear in a fairly constant range 1400—1460 cm^{-1} [60]. The observed strong and weak IR bands at 1479 cm^{-1} and 1464 cm^{-1} are assigned to the CH_3 bending modes ν_{10}, ν_{11}, ν_{34}, and ν_{35} being in good agreement with the calculated modes at 1498 cm^{-1}, 1488 cm^{-1}, 1481 cm^{-1}, and 1457 cm^{-1} and with earlier studies [60, 61]. Moreover, the umbrella modes (ν_{12} and ν_{13}) match the observed weak and strong IR bands at 1448 cm^{-1} and 1434 cm^{-1}, respectively being in agreement with the predicted IR intensities of 6.8 km/mol and 145.8 km/mol, respectively. Four methyl rocking modes of two methyl groups (ρCH_3; ν_{20}, ν_{21} and ν_{36}, ν_{37} are predicted at 1116 cm^{-1}, 1032 cm^{-1} and 1137 cm^{-1}, 1128 cm^{-1}, respectively) were observed at 1139 cm^{-1} for ν_{36}, ν_{37}, ν_{20} and 1004 cm^{-1} for ν_{21} in the IR spectrum respectively being in agreement with the literature values of 1140 cm^{-1}, 1088 cm^{-1}, 1014 cm^{-1}, and 994 cm^{-1} [62—64]. The CH_3 torsion modes (ν_{45} and ν_{46}) were predicted at 125 cm^{-1} and 114 cm^{-1} respectively, but were not expected to be observed because of the Rayleigh scattering background below 400 cm^{-1} (Fig. 3).

C=O fundamental vibrations. In the titled compound we have two C=O groups; the C=O stretching frequency appears strongly in the FT-IR spectrum in the range 1850—1600 cm^{-1}. Normally carbonyl group vibrations occur in the range 1780—1680 cm^{-1} [65]. Thus, very strong bands at 1709 cm^{-1} and 1670 cm^{-1} in the IR spectrum are assigned to C=O stretching vibrations. These bands are in concurrence with the predicted IR intensities of 170.4 km/mol and 780.1 km/mol, respectively. One of the C=O in-plane bending modes (ν_{26}) is assigned to a weak IR band at 602 cm^{-1} which is consistent with the previous study [66]. The other C=O in-plane bending mode (ν_{29}) is computed at 396 cm^{-1} by the B3LYP method. They are absent in the IR spectrum because they were beyond the detection capability of the experimental facilities (below 400 cm^{-1}). Moreover, the C=O out-of-plane bending vibrations (ν_{40}, ν_{41}) are calculated at 748 cm^{-1} and 707 cm^{-1}. These bands are assigned to the observed strong bands at 762 cm^{-1} and 728 cm^{-1} (Table 3).

Ring fundamental vibrations. The C=C and C—C stretching vibrations were predicted at 1600 cm^{-1} and 982 cm^{-1} by the B3LYP method. These computed data are slightly different from the experimental strong and weak IR bands at 1616 cm^{-1} and 955 cm^{-1} and are in good agreement with the predicted IR intensities of 53.1 km/mol and 21.7 km/mol, respectively. The ring deformation modes ν_{24}, ν_{27}, and ν_{28} calculated at 780 cm^{-1}, 496 cm^{-1}, and 464 cm^{-1} were assigned to the observed bands at 799 cm^{-1}, 522 cm^{-1}, and 481 cm^{-1} respectively. These assignments are in good agreement with the literature data [35, 67]. On the other hand, the ring puckering modes ν_{42}, ν_{47}, and ν_{48} were beyond the detection capability of the experimental facilities.

The identification of C—N vibrations is a difficult task since the mixing of vibrations is possible in this rang [59]. It is worth noting that the observed band at 1376 cm^{-1} assigned to the C—N stretch (ν_{15}) was computed at 1361 cm^{-1}. Moreover, the observed strong, weak, and medium IR bands at 1342 cm^{-1}, 1231 cm^{-1}, and 1174 cm^{-1} match the predicted IR intensities of 75.9 km/mol, 1.4 km/mol, and 17.7 km/mol. These bands were assigned to CN stretches ν_{16}, ν_{17}, and ν_{18}. The other two CN stretches (ν_{23} and ν_{25}) were assigned to weak IR bands at 932 cm^{-1} and 685 cm^{-1}, respectively, in agreement with the previous investigations [12, 35, 61].

CONCLUSIONS

The theoretical calculations and the IR spectrum favors *diketo* 1,3-dimethyluracil (structure **3**) in the solid phase, which is consistent with the normal coordinate analysis and vibrational frequency calculations. Confident vibrational assignments for all observed bands to their corresponding fundamentals have been proposed.

U.A. Soliman sincerely thanks Prof. T.A. Mohamed, Department of Chemistry, Al-Azhar University (Men′s Campus), Nasr City 11884, Cairo, Egypt for providing the opportunity to use the Gaussian 98 program. Deep thanks go also to Prof. J.R. Durig, Chemistry Department, College of Arts and Sciences, University of Missouri, Kansas City, MO 64110, USA for the complementary programs to calculate FCs and PEDs.

REFERENCES

1. *Krishnakumar V., Xavier R.J.* // Indian J. Pure Appl. Phys. – 2003. – **41**. – P. 597 – 601.
2. *Contreras J.G., Seguel G.V.* // Spectrochim. Acta. – 1992. – **48A**. – P. 525 – 532.
3. *Contreras J.G., Seguel G.V.* // Bol. Soc. Chil. Quim. – 1982. – **27**. – P. 5 – 8.
4. *Sundaraganesan N., Kumar K.S., Meganathan C., Joshua B.D.* // Spectrochim. Acta. – 2006. – **65A**. – P. 1186 – 1196.
5. *Balci K., Akyuz S.* // J. Mol. Struct. – 2005. – **744-747**. – P. 909 – 919.
6. *Subramanian M.K., Anbarasan P.M., Manimegalai S.* // Spectrochim. Acta. – 2009. – **73A**. – P. 642 – 649.
7. *Arivazhagan M., Rexalin D.A.* // Spectrochim. Acta, Part A: Mol. Biomol. Spectrosc. – 2013. – **107**. – P. 347 – 358.
8. *Jain K.S., Chitre T.S., Miniyar P.B., Kathiravan M.K., Bendre V.S., Veer V.S., Shahane S.K., Shishore C.J.* // Curr. Sci. – 2006. – **90**, N 6. – P. 793 – 803.
9. *Ito M., Shimada R., Kuraishi T., Mizushima W.* // J. Chem. Phys. – 1956. – **25**. – P. 597/598.
10. *Lord R.C., Marston A.L., Miller F.A.* // Spectrochim. Acta. – 1957. – **9**. – P. 113 – 125.
11. *Breda S., Reva I.D., Lapinski L., Nowak M.J., Fausto R.* // J. Mol. Struct. – 2006. – **786**. – P. 193 – 206.
12. *Lukmanov T., Ivanov S.P., Khamitov E.M., Khursan S.L.* // Comput. Theoret. Chem. – 2013. – P. 38 – 45.
13. *Schoellhorn H., Thewalt U., Lippert B.* // J. Am. Chem. Soc. – 1989. – **111**, N 18. – P. 7213 – 7221.
14. *Balachandran V., Parimala K.* // Spectrochim. Acta Part A: Mol. Biomol. Spectrosc. – 2013. – **102**. – P. 30 – 51.
15. *Masunov A.E., Grischenko S.I., Zorkiy P.M.* // Zh. Fiz. Khim. – 1993. – **67**. – P. 221.
16. *Bane1liee A., Dattagupta J.K., Saenger W., Raaczenko A.* // Acta Crystallogr. – 1977. – **B33**. – P. 90 – 94.
17. *Brown R.D., Godfrey P.D., McNaughton D., Pierlot A.P.* // J. Am. Chem. Soc. – 1988. – **110**, N 7. – P. 2329 – 2330.
18. *Beak P., White J.M.* // J. Am. Chem. Soc. – 1982. – **104**, N 25. – P. 7073 – 7077.
19. *Katritzky A.R., Baykut G., Rachwal S., Szafran M., Caster K.C., Eyler J.* // J. Chem. Soc., Perkin Trans. 2. – 1989. – N 10. – P. 1499 – 1506.
20. *Pulay P.* // Mol. Phys. – 1969. – **17**. – P. 197 – 204.
21. *Moller C., Plesset M.S.* // Phys. Rev. – 1934. – **46**. – P. 618 – 622.
22. *Parr R.G., Yang W.* Density-Functional Theory of Atoms // Molecules, Oxford University Press, New York, 1989.
23. *Becke A.D.* // J. Chem. Phys. – 1993. – **98**. – P. 5648 – 5652.
24. *Vosko S.H., Wilk L., Nusair M.* // Canad. J. Phys. – 1980. – **58**. – P. 1200 – 1211.
25. *Lee C., Yang W., Parr R.G.* // Phys. Rev. – 1988. – **37B**. – P. 785 – 789.
26. *Becke A.D.* // Phys. Rev. – 1988. – **38A**. – P. 3098 – 3100.
27. *Frisch M.J., Trucks G.W., Schlegel H.B., Scuseria G.E., Robb M.A., Cheeseman J.R., Zakrzewski V.G., Montgomery J.A. Jr., Stratmann R.E., Burant J.C., Dapprich S., Millam J.M., Daniels A.D., Kudin K.N., Strain M.C., Farkas O., Tomasi J., Barone V., Cossi M., Cammi R., Mennucci B., Pomelli C., Adamo C., Clifford S., Ochterski J., Petersson G.A., Ayala P.Y., Cui Q., Morokuma K., Malick D.K., Rabuck A.D., Raghavachari K., Foresman J.B., Cioslowski J., Ortiz J.V., Baboul A.G., Stefanov B.B., Liu G., Liashenko A., Piskorz P., Komaromi I., Gomperts R., Martin R.L., Fox D.J., Keith T., Al-Laham M.A., Peng C.Y., Nanayakkara A., Gonzalez C., Challacombe M., Gill P.M.W., Johnson B., Chen W., Wong M.W., Andres J.L., Gonzalez C., Head-Gordon M., Replogle E.S., Pople J.A.* Gaussian 98, Revision A.7. – Pittsburgh, PA: Gaussian Inc., 1998.
28. *Dennington R., Keith T., Millam J.* Gauss View, Version 5. – Shawnee Mission, KS, Semichem Inc., 2009.
29. *Subashini A., Muthiah P.T., Lynch D.E.* // Acta Crystallogr., Sect. E. – 2008. – **64**. – P. o426.
30. *Melandri S., Sanz M.E., Caminati W., Favero P.G., Kisiel Z.* // J. Am. Chem. Soc. – 1998. – **120**. – P. 11504 – 11509.
31. *Wilson E.B., Decius J.C., Cross P.C.* Molecular Vibrations. – New York: McGraw-Hill, 1955.
32. *Balachandran V., Lakshmi A., Janaki A.* // Spectrochim. Acta, Part A. – 2011. – **81**. – P. 1 – 7.
33. *Schachtschneider J.H.* Vibrational Analysis of Polyatomic Molecules. Parts 5 and 6, tech. rep. Nos. 231 and 57, Shell Development Co., Houston, TX, 1964 and 1965.

34. *Sinha P., Boesch S.E., Gu C., Wheeler R.A., Wilson A.K.* // J. Phys. Chem. Part A. – 2004. – **108**. – P. 9213 – 9217.
35. *Yamaguchi Y., Frisch M., Gaw J., Schaefer H.F. III, Binkley J.S.* // J. Chem. Phys. – 1986. – **84**. – P. 2262 – 2278.
36. *Bondi A.* // J. Phys. Chem. – 1964. – **68**. – P. 441 – 451.
37. *Pulay P., Zhou X., Fogarasi G.* in: Recent Experimental, Computational Advances in Molecular Spectroscopy. – The Netherlands: Kluwer Acad. Publ., 1993. – P. 99.
38. *Palafox M.A., Rastogi V.K.* // Spectrochim. Acta. – 2000. – **58A**. – P. 411 – 440.
39. *Mohamed T.A.* // J. Mol. Struct.: THEOCHEM. – 2005. – **713**. – P. 179 – 192.
40. *Mohamed T.A., Aly M.M.A.* // J. Raman Spectrosc. – 2004. – **35**. – P. 869 – 878.
41. *Soliman U.A., Hassan A.M., Mohamed T.A.* // Spectrochim. Acta, Part A. – 2007. – **68**. – P. 688 – 700.
42. *Chantry G.W.* in: Raman Effect, A. Anderson (ed.), vol. 1. – NY: Marcel Dekker Inc., 1971, ch. 2.
43. *Amos R.D.* // Chem. Phys. Lett. – 1986. – **124**. – P. 376 – 381.
44. *Polavarapu P.L.* // J. Phys. Chem. – 1990. – **94**. – P. 8106 – 8112.
45. http: // sdbs.db.aist.go.jp/sdbs/cgi-bin/direct_frame_disp.cgi?sdbsno=563.
46. *David J.G., Hallam H.S.* // Spectrochim. Acta. – 1965. – **21**. – P. 841 – 850.
47. *Krueger P.J.* // Tetrahedron. – 1970. – **26**. – P. 4753 – 4764.
48. *Arivazhagan M., Meenakshi R.* // Spectrochim. Acta, Part A: Mol. Biomol. Spectrosc. – 2012. – **91**. – P. 419 – 430.
49. *Durig J.R., Church J.S.* // Spectrochim. Acta, Part A. – 1980. – **36**. – P. 957 – 964.
50. *Socrates G.* Infrared, Raman Characteristic Group Frequencies, Tables, Charts, 3rd ed. – Chichester: John Wiley, Sons, 2001.
51. *Dwivedi P., Sharma S.N.* // Indian J. Pure Appl. Phys. – 1973. – **11**. – P. 447 – 451.
52. *Varsanyi G.* Assignments for Vibrational Spectra of Seven Hundred Benzene Derivatives, vols. 1/2, Addam Hilger, 1974.
53. *Singh N.P., Yadav R.A.* // Indian J. Phys. – 2001. – **B75**. – P. 347.
54. *Balachandran V., Parimala K.* // J. Mol. Struct. – 2012. – **1007**. – P. 136 – 145.
55. *Jag M.* Organic Spectroscopy — Principles, Application, 2nd ed. – New Delhi: Narosa Publication House, 2010.
56. *Alpert N.L., Keiser W.E., Szymanski H.A.* Theory, Practice of Infrared Spectroscopy. – Plenum/Rosetta, New York, 1973.
57. *Sundaraganesan N., Meganathan C., Kurt M.* // J. Mol. Struct. – 2008. – **891**. – P. 284 – 291.
58. *Baruah R., Amma A., Dube P.S., Rai S.N.* // Indian J. Pure Appl. Phys. – 1970. – **8**. – P. 761.
59. *Silverstein M., Basseler G.C., Morill C.* Spectrometric Identification of Organic Compounds. – New York: Wiley, 1981.
60. *Sundaraganesan N., Saleem H., Mohan S., Ramalingam M., Sethuraman V.* // Spectrochim. Acta, Part A. – 2005. – **62**. – P. 740 – 751.
61. *Mohamed T.A., Hassan A.M., Soliman U.A., Zoghaib W.M., Husband J., Hassan S.M.* // Spectrochim. Acta, Part A. – 2011. – **79**. – P. 1722 – 1730.
62. *Green J.H.S., Harrison D.J., Kynbaston W.* // Spectrochim. Acta, Part A. – 1971. – **27**. – P. 793 – 806.
63. *Susi H., Ard J.S.* // Spectrochim. Acta, Part A. – 1974. – **30**. – P. 1843 – 1853.
64. *Goel R.K., Gupta S.P., Agarwal M.L., Sharma S.N.* // Indian J. Pure Appl. Phys. – 1981. – **19**. – P. 501.
65. *Mohan J.* Organic Spectroscopy-Principle, Applications, 2nd ed. – New Delhi: Narosa Publishing House, 2000. – P. 30 – 32.
66. *Roeges N.P.G.* Guide to The Interpretation of Infrared Spectra of Organic Structures. – Chichester: John Wiley, Sons, 1994.
67. *Sathiyanarayanan D.N.* Vibrational Spectroscopy Theory, Application. – New Delhi: New Age International Publishers, 2004.